RESEARCH PAPER

Formulation and In Vitro Characterization of a Troxerutin-Loaded Chitosan–Xanthan Gum Scaffold for Cartilage Regeneration

Shaik Saddam Hussain .[1], Shanmugarajan T.S.[2]*

[1] Research Scholar, Department of Pharmaceutics, School of Pharmaceutical Sciences, Vels Institute of Science, Technology and Advanced Studies (VISTAS), PV Vaithiyalingam Rd, Velan Nagar, Krishnapuram, Pallavaram, Chennai, Tamil Nadu 600117.

[2] Professor, Department of Pharmaceutics, School of Pharmaceutical Sciences, Vels Institute of Science, Technology and Advanced Studies (VISTAS), PV Vaithiyalingam Rd, Velan Nagar, Krishnapuram, Pallavaram, Chennai, Tamil Nadu 600117.

Corresponding author: smrajan.sps@vistas.ac.in

ABSTRACT

This study aimed to develop and characterize a troxerutin-loaded chitosan–xanthan gum scaffold for sustained local delivery and potential application in cartilage regeneration. Five scaffold formulations, namely CD, XD, CXD, CXHD and CDX, were prepared using chitosan and xanthan gum, with troxerutin incorporated into the polymeric matrix. The formulations were evaluated by scanning electron microscopy (SEM), drug content, encapsulation efficiency, particle size, zeta potential, Fourier transform infrared spectroscopy (FTIR), differential scanning calorimetry (DSC), X-ray diffraction (XRD), swelling, biodegradation, in vitro drug release and release kinetics. Among the formulations, CDX exhibited the most porous, interconnected and uniform architecture and was selected as the optimized formulation. The optimized scaffold contained 656.21 ± 11.82 µg troxerutin per 5 mg scaffold, with an encapsulation efficiency of 92.56 ± 5.10% and drug loading of 53.12 ± 1.45%. The mean particle size was 440 ± 28.6 nm and the zeta potential was −9.0 ± 7.6 mV. The scaffold showed a swelling index of 278.57 ± 12.34% at 1 h, increasing to 392.85 ± 17.11% at 24 h, while degradation reached 62.7 ± 1.2% at 7 days. Overall, the CDX scaffold demonstrated a combination of porous architecture, high swelling capacity that supports its further investigation as a candidate biomaterial for cartilage tissue engineering.

Keywords: Troxerutin; Chitosan; Xanthan gum; Scaffold; Cartilage regeneration; Sustained drug release; Tissue engineering; Antioxidant; Anti-inflammatory

How to cite this article: Shaik Saddam Hussain .. Formulation and In Vitro Characterization of a Troxerutin-Loaded Chitosan–Xanthan Gum Scaffold for Cartilage Regeneration. Int J Drug Deliv Technol. 2026;16(7):1011-1015. DOI: 10.25258/ijddt.16.7.107

INTRODUCTION

Cartilage regeneration remains challenging because articular cartilage has limited intrinsic regenerative capacity. [7,13] An effective tissue-engineering scaffold should provide a three-dimensional environment capable of supporting cell attachment, nutrient transport, extracellular matrix deposition and localized delivery of bioactive agents. [3,13] Porous polymeric scaffolds are therefore attractive for cartilage repair because their architecture can facilitate fluid exchange and tissue interaction. [6,11]

Chitosan is a biocompatible, hydrophilic polysaccharide with film-forming and tissue-engineering properties, whereas xanthan gum is an anionic polysaccharide that can contribute to hydration, structural organization and matrix stability. [2,4,9] Their combination can generate a polyelectrolyte complex through interactions between protonated amino groups of chitosan and carboxyl groups of xanthan gum. [2,9] Such interactions can influence scaffold porosity, swelling, drug retention and structural integrity. [4,9]

Troxerutin is a flavonoid glycoside with antioxidant and anti-inflammatory properties. [8,15] These characteristics make it of interest for biomaterial systems intended for inflammatory and degenerative tissue conditions. [8,15] However, incorporation of a bioactive compound into a polymeric scaffold is important for maintaining local exposure and controlling its release. [1,5] A chitosan–xanthan gum matrix may provide a hydrated, porous environment for prolonged drug delivery. [2,9]

The present study was undertaken to formulate and characterize troxerutin-loaded chitosan–xanthan gum scaffolds and to identify an optimized formulation based on morphological and physicochemical characteristics. The optimized scaffold was further evaluated for drug loading, surface charge, structural compatibility, thermal and crystalline behavior, swelling, biodegradation,

2. MATERIALS AND METHODS

2.1 Preparation of Troxerutin-Loaded Scaffolds

Chitosan was dissolved in 1% w/v acetic acid to obtain a clear polymer solution. Xanthan gum was separately dissolved in distilled water under continuous stirring at 700 rpm for 1 h. The polymer solutions were mixed for 2 h under constant stirring to obtain a uniform polymer blend. Troxerutin was dissolved in DMSO and gradually incorporated into the polymer mixture under continuous stirring for 6 h to facilitate uniform distribution of the drug throughout the matrix.

2.2 Formulation Screening and Selection of the Optimized Scaffold

Five formulations were prepared and designated CD (chitosan + troxerutin), XD (xanthan gum + troxerutin), CXD (chitosan + xanthan gum + troxerutin), CXHD (chitosan + xanthan gum + troxerutin with heat treatment), and CDX (chitosan + troxerutin + xanthan gum). The formulations were compared on the basis of surface morphology and pore architecture. The formulation showing the most desirable porous,

interconnected and uniform structure was selected for detailed characterization.

2.3 Scanning Electron Microscopy

Lyophilized scaffold samples were mounted on double-sided adhesive carbon tape fixed to aluminum stubs and sputter-coated with a thin layer of gold. The coated samples were examined by SEM at different magnifications under suitable accelerating voltage to evaluate surface morphology and pore architecture.

2.4 Standard Curve and Drug Content

Standard curves were prepared in DMSO (2–12 µg/mL) and phosphate buffer pH 7.4 (0–15 µg/mL) using a 1 mg/mL stock solution. Absorbance was measured at 355 nm by UV–Visible spectrophotometry. For drug-content determination, a known amount of scaffold was dissolved in DMSO, filtered to remove insoluble polymer and diluted before measurement at 355 nm.

2.5 Encapsulation Efficiency and Drug Loading

The formulation was centrifuged at 15,000 rpm for 30 min and the supernatant containing free drug was analyzed by UV spectrophotometry. Entrapped drug was calculated as total drug minus free drug. Encapsulation efficiency and drug loading were calculated from the measured drug quantities.

2.6 Particle Size and Zeta Potential

The optimized CDX formulation was diluted with distilled water and sonicated before particle-size measurement by dynamic light scattering at 25°C. Zeta potential was measured using electrophoretic mobility at 25°C after dilution in deionized water.

2.7 FTIR, DSC and XRD

FTIR was used to evaluate compatibility among troxerutin, chitosan and xanthan gum. Samples were dried, ground and prepared with KBr, and spectra were recorded over 4000–400 cm^{-1}. DSC was performed using 5–10 mg samples heated from 10 to 500°C at 10°C/min under nitrogen. XRD patterns were recorded using Cu-Kα radiation over a 2θ range of 5–80° to assess crystallinity and the physical state of troxerutin.

2.8 Swelling and Biodegradation

For swelling studies, dry scaffold weight (W_0) was recorded before immersion in phosphate buffer pH 7.4. At predetermined intervals the scaffold was removed, surface liquid was gently blotted and the swollen weight (W_t) was recorded. Swelling index was calculated as $[(W_t - W_0)/W_0] \times 100$. Biodegradation was evaluated in PBS at 37°C, with the degradation medium changed every 2 days and percentage weight loss determined at specified time points up to 7 days.

2.9 Statistical Analysis

The source scaffold document reports comparative formulation observations and fitted release models. No complete numerical ANOVA dataset or p-values were provided in the scaffold results; therefore, no additional statistical significance values have been introduced in this manuscript.

3. RESULTS AND DISCUSSION

3.1 Optimization by SEM

Five formulations were evaluated to identify a scaffold with suitable morphology for tissue-engineering applications. CD exhibited a relatively dense structure with fewer interconnected pores, consistent with the film-forming nature of chitosan. XD showed irregular and poorly organized pores, indicating that xanthan gum alone did not provide the desired three-dimensional architecture. CXD showed improved pore formation following interaction between chitosan and xanthan gum. CXHD exhibited partial structural collapse and merging of pore walls, which was attributed in the source report to heat-induced changes in polymer organization. In contrast, CDX demonstrated the most porous, interconnected and uniform structure, with an even pore distribution and no visible crystalline aggregates. CDX was therefore selected as the optimized formulation.

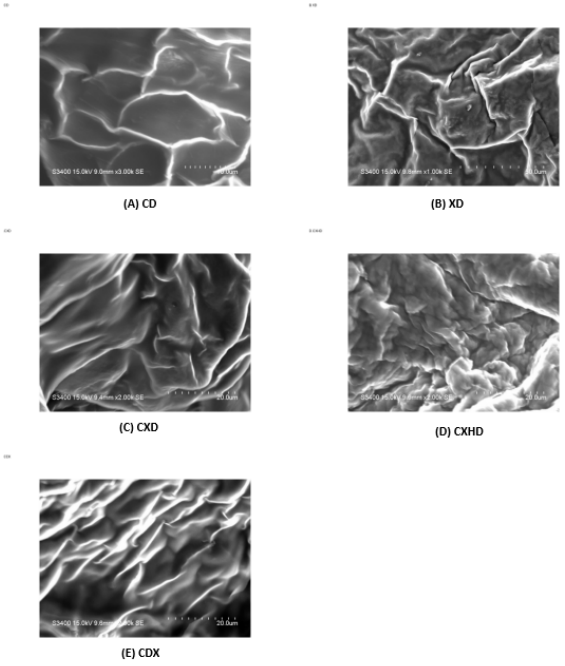

Figure 1. Scanning electron microscopy images of the five scaffold formulations: (A) CD, (B) XD, (C) CXD, (D) CXHD and (E) CDX. CDX showed the most porous, interconnected and uniform architecture and was selected as the optimized formulation.

3.2 Drug Content, Encapsulation Efficiency and Drug Loading

UV–Visible analysis at 355 nm showed that 5 mg of the optimized CDX scaffold contained 656.21 ± 11.82 µg of troxerutin, demonstrating successful incorporation and relatively uniform drug distribution. The encapsulation efficiency was 92.56 ± 5.10%, while drug loading was 53.12 ± 1.45%. The high encapsulation efficiency was attributed in the source report to polymer–drug interactions and the dense polyelectrolyte network formed by chitosan and xanthan gum.

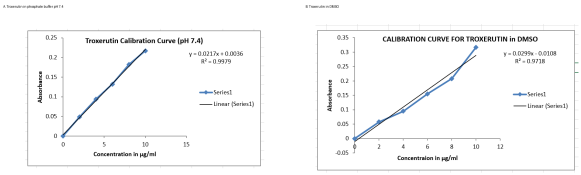

Figure 2. Calibration curves of troxerutin measured by UV–Visible spectrophotometry at 355 nm: (A) phosphate buffer pH 7.4 and (B) DMSO.

3.3 Particle Size and Zeta Potential

The optimized formulation showed a mean particle size of 440 ± 28.6 nm. The reported PDI was described as being close to 1, indicating moderate heterogeneity. The zeta potential was −9.0 ± 7.6 mV. The slightly negative surface charge was interpreted as partial neutralization of chitosan's positively charged amino groups through interaction with xanthan gum and troxerutin, supporting formation of the polyelectrolyte complex.

Figure 3. Characterization of the optimized CDX formulation by dynamic light scattering: (A) particle-size distribution and (B) zeta-potential profile.

3.4 FTIR Analysis

FTIR analysis supported compatibility among the formulation components. Chitosan showed characteristic bands around 3439.66 cm^{-1} associated with overlapping O–H/N–H stretching, together with bands near 1638.96 and 1605 cm^{-1}. Xanthan gum showed a hydroxyl band around 3424.85 cm^{-1} and a carboxylate band around 1629 cm^{-1}. The optimized CDX scaffold exhibited broadening and shifting around 3400 cm^{-1}, consistent with intermolecular hydrogen bonding and interaction among chitosan, xanthan gum and troxerutin. The absence of additional unexpected peaks supported successful incorporation without evidence of major chemical incompatibility.

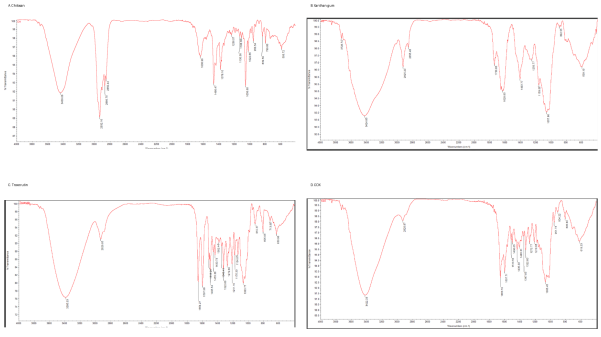

Figure 4. FTIR spectra of the formulation components and optimized scaffold: (A) chitosan, (B) xanthan gum, (C) troxerutin and (D) CDX.

3.5 DSC Analysis

Pure troxerutin showed a sharp endothermic melting peak at 179.4°C, characteristic of its crystalline state. In the optimized scaffold, the characteristic drug endotherm was markedly reduced and appeared around 171°C. This change was interpreted as evidence of reduced crystallinity and possible amorphous or molecularly dispersed drug within the polymeric matrix.

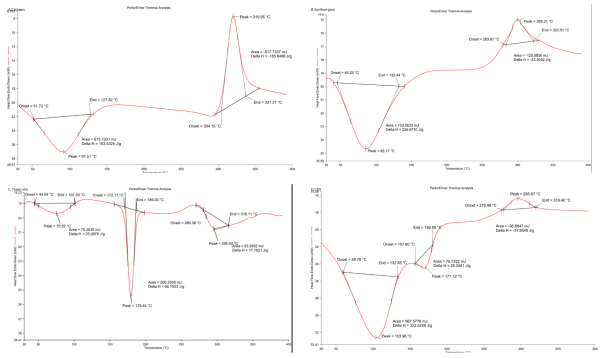

Figure 5. DSC thermograms of the formulation components and optimized scaffold: (A) chitosan, (B) xanthan gum, (C) troxerutin and (D) CDX.

3.6 XRD Analysis

Pure troxerutin displayed defined crystalline diffraction peaks, while chitosan showed a semi-crystalline pattern and xanthan gum was predominantly amorphous. The CDX scaffold showed a broad halo with a marked reduction in characteristic troxerutin peaks. The XRD findings were consistent with DSC and supported a reduction in drug crystallinity following incorporation into the polymeric matrix.

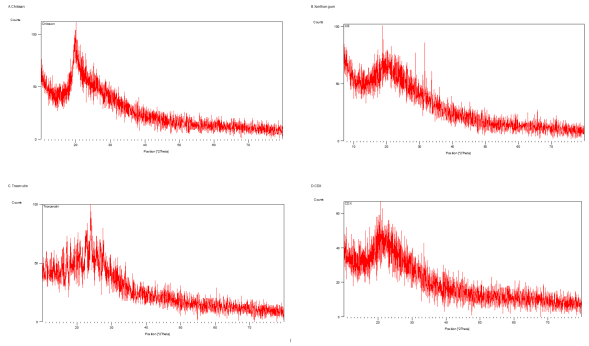

Figure 6. XRD diffractograms of the formulation components and optimized scaffold: (A) chitosan, (B) xanthan gum, (C) troxerutin and (D) CDX.

3.7 Swelling Behavior

The optimized scaffold showed a swelling index of 278.57 ± 12.34% at 1 h, which increased to 392.85 ± 17.11% at 24 h. The scaffold retained its overall structure during the one-week experimental observation period. The high water uptake is consistent with the hydrophilic nature of chitosan and xanthan gum and the presence of hydroxyl, amino and carboxyl groups capable of interacting with water.

3.8 Biodegradation

The scaffold exhibited 11.24 ± 0.45% degradation at 24 h and 62.7 ± 1.2% at 7 days. The gradual loss of mass

was interpreted as a consequence of the hydrophilic nature of xanthan gum and progressive disentanglement of the chitosan–xanthan gum network. The observed degradation profile was considered compatible with the requirement for a scaffold to maintain structural integrity while permitting gradual matrix breakdown.

The optimized CDX scaffold combines a porous and interconnected architecture with high water uptake and sustained drug release. The SEM findings suggest that the scaffold provides a three-dimensional network that can facilitate fluid movement and potentially support cellular interactions. The swelling behavior further demonstrates the ability of the matrix to absorb and retain aqueous medium, an important characteristic for hydrated tissue-engineering environments.

The high encapsulation efficiency and drug loading indicate effective incorporation of troxerutin within the chitosan–xanthan gum network. FTIR findings support intermolecular interactions and polyelectrolyte complex formation, while DSC and XRD indicate reduced crystallinity of troxerutin in the scaffold. These changes may be favorable for maintaining the drug in a dispersed state within the polymeric matrix, although improved solubility or bioavailability should be confirmed experimentally rather than inferred solely from solid-state characterization. Taken together, the CDX scaffold showed a favorable combination of porous morphology, hydration capacity, drug incorporation, controlled release and retained biological activity. These characteristics justify further studies involving mechanical strength, cytocompatibility, chondrocyte or mesenchymal stem-cell responses, extracellular matrix deposition and appropriate animal models before any translational claims are made.

4. CONCLUSION

A troxerutin-loaded chitosan–xanthan gum scaffold was successfully developed and characterized. Among the evaluated formulations, CDX demonstrated the most favorable porous and interconnected morphology and was selected as the optimized formulation. The scaffold showed high encapsulation efficiency (92.56 ± 5.10%), drug loading (53.12 ± 1.45%), substantial swelling capacity and progressive biodegradation. Overall, the optimized CDX scaffold represents a promising experimental biomaterial platform for localized troxerutin delivery and warrants further in vitro cellular and in vivo studies focused specifically on cartilage regeneration and safety.

5. CONFLICT OF INTEREST

The authors declare no conflict of interest.

6. ACKNOWLEDGEMENT

The authors acknowledge Vels Institute of Science, Technology and Advanced Studies (VISTAS) for providing facilities and institutional support for the study.

7. REFERENCES

1. Abou-Okeil A, Taha GM. Investigation and kinetics of hydrogel scaffold with sustained release ciprofloxacin hydrochloride. Polymer Bulletin. 2024;81(18):17393–17411.

2. Almeida HH, Santamaria-Echart A, Amaral JS, Aquino LL, Rodrigues AE, Barreiro MF. Chitosan-xanthan gum-based hydrogels loaded with essential oil distillation by-products of Aloysia citrodora Paláu for antimicrobial systems. International Journal of Biological Macromolecules. 2026;150368.

3. Burke G, Barron V, Geever T, Geever L, Devine DM, Higginbotham CL. Evaluation of the materials properties, stability and cell response of a range of PEGDMA hydrogels for tissue engineering applications. Journal of the Mechanical Behavior of Biomedical Materials. 2019;99:1–10.

4. de Andrade LRM, Mota WS, de Melo Barbosa R, Cardoso JC, Andrade LN, Pereira MM, et al. Synthesis and characterization of a new biomaterial-based scaffold based on chitosan and cashew gum: an inquiry into structural and physical properties. Journal of Porous Materials. 2025;32(1):203–215.

5. Gu B, Qi J, Li X, Wang S, Ma Y, Zhang J, Ma T. Intra-articular targeted delivery of nanomaterials for the treatment of osteoarthritis: focusing on cell signaling pathway mechanisms. Expert Opinion on Drug Delivery. 2026;23(4):643–659.

6. Karaca I, Aldemir Dikici B. Quantitative evaluation of the pore and window sizes of tissue engineering scaffolds on scanning electron microscope images using deep learning. ACS Omega. 2024;9(23):24695–24706.

7. Krakowski P, Rejniak A, Sobczyk J, Karpiński R. Cartilage integrity: A review of mechanical and frictional properties and repair approaches in osteoarthritis. Healthcare. 2024;12(16):1648.

8. Lee GB, Kim Y, Lee KE, Vinayagam R, Singh M, Kang SG. Anti-inflammatory effects of quercetin, rutin, and troxerutin result from the inhibition of NO production and the reduction of COX-2 levels in RAW 264.7 cells treated with LPS. Applied Biochemistry and Biotechnology. 2024;196(12):8431–8452.

9. Malik NS, Ahmad M, Minhas MU, Tulain R, Barkat K, Khalid I, Khalid Q. Chitosan/xanthan gum based hydrogels as potential carrier for an antiviral drug: fabrication, characterization, and safety evaluation. Frontiers in Chemistry. 2020;8:510555.

10. Patel Rajesh M, Patel Natvar J. In vitro antioxidant activity of coumarin compounds by DPPH, super oxide and nitric oxide free radical scavenging methods. Journal of Advanced Pharmacy Education & Research. 2011;1(1):52–68.

11. Patole V, Kavitkar G, Ingavle G, Behere I, Wavhale R, Jha A, et al. Calcium phosphate reinforced chitosan–carrageenan scaffolds: characterization and in vitro assessment for wound healing. RSC Pharmaceutics. 2025;2(4):772–791.

12. Raoufi Z, Abdollahi S. Development of Gelatin/Shekar tighal/Persian gum-based films reinforced with Anghozeh oil for potential wound dressing applications. Polymer Bulletin. 2024;81(9):8405–8424.

13. Rawojć K, Tadeusiewicz R, Zych-Stodolak E. Advancements in Chitosan-based scaffolds for chondrogenic differentiation and knee cartilage regeneration: current trends and future perspectives. Bioengineering. 2025;12(7):740.
14. Subi TM, Selvasudha N, Priyadharshini S, Kumar P, Singh R, Vasanthi HR. Antibacterial, antifungal, and cytotoxic potential of plumbagin-loaded pH-responsive vaginal nanoformulations. Applied Biochemistry and Biotechnology. 2024;196(12):8763–8790.
15. Subbaraj GK, Elangovan H, Chandramouli P, Yasam SK, Chandrasekaran K, Kulanthaivel L, et al. Antiangiogenic potential of troxerutin and chitosan loaded troxerutin on chorioallantoic membrane model. BioMed Research International. 2023;2023:5956154.
16. Vyas C. Development of a multi-material and multi-scale 3D bioprinted scaffold for osteochondral tissue engineering. University of Manchester; 2019.
17. Wei J, Liu J, Wu J, Chen Y, Wei K, Guo J, Su Z. Preparation and osteogenic performance study of troxerutin-loaded carboxymethyl cellulose/Si-calcium phosphate cement composite bone cement. Biomaterials Advances. 2025;214434.